JOC Article

Self-Assembling of the Porphyrin-Linked Acyclic Penta- and Heptapeptides in Aqueous Trifluoroethanol

Toru Arai,*,§ Makiko Inudo,‡ Tomomi Ishimatsu,‡ Chieko Akamatsu,‡ Yasushi Tokusaki,‡ Tomikazu Sasaki,# and Norikazu Nishino$

Institute for Fundamental Research of Organic Chemistry, Kyushu University, Fukuoka, 812-8581, Japan, Faculty of Engineering, Kyushu Institute of Technology, Kitakyushu, 804-8550, Japan, Department of Chemistry, University of Washington, Seattle, Washington 98195, and Graduate School of Life Science and Systems Engineering, Kyushu Institute of Technology, Kitakyushu, 808-0196, Japan

arai@che.kyutech.ac.jp

Received January 2, 2003

The conjugates of porphyrin with links to the acyclic penta- and heptapeptides were synthesized to mimic natural multiple porphyrin systems. The linear penta- and heptapeptide with hydrophilic/hydrophobic alternative sequences took a random structure in aqueous trifluoroethanol (TFE). However, these polypeptides took a β-sheet structure in the same solvent when the N-terminal Cys linked to the porphyrin, suggesting that the conjugates self-assembled via the intermolecular hydrophobic interaction between the porphyrins. The circular dichroism (CD) spectra, UV/vis spectra, size exclusion chromatography (SEC), and ^{1}H NMR spectroscopy supported the self-assembling. In the self-assembled structure of the pentapeptide linking porphyrin at the *p*-phenyl position (**9**), the porphyrins were involved in two porphyrin−porphyrin interactions, i.e., the side-by-side interaction between the neighboring polypeptide chains and the face-to-face interaction between the first and the third peptide chains. The CD spectra of **9** showed two sets of Cotton effects probably arising from these two interactions. The UV/vis spectra also supported the above interpretation, showing multiple absorptions in the longwave and shortwave shifted regions. The SEC analyses showed the assembled structure of the conjugates. The ^{1}H NMR signals of the porphyrin rings of **9** were hardly observed in D_2O-CD_3OD because of the shortened spin−spin relaxation time T_2.

Introduction

The clusters of porphyrin derivatives often perform an excellent photochemistry in living systems. The bacterial photosynthetic reaction center consists of two bachteriochloropylls as a special pair with several pigments located nearby.[1] In the light-harvesting complex II of *Rhodopseudomonas acidophila*, a number of bachteriochlorophylls form ring-shaped structures.[2] Also, multiple porphyrins (hemes) play different roles with each other in some redox enzymes.[3] Thus, the complex multipigment assemblies have attracted a great deal of attention, therefore, synthetic organic chemists are required to construct more and more complex molecules as models. For this purpose, covalently linked dimeric[4] and oligomeric[5−7] porphyrins have been synthesized. The strategy of supramolecular chemistry also afforded the multipor-

§ Kyushu University. Present address: Faculty of Engineering, Kyushu Institute of Technology.
‡ Faculty of Engineering, Kyushu Institute of Technology.
# University of Washington.
$ Graduate School of Life Science and Systems Engineering, Kyushu Institute of Technology.

(1) Deisenhofer, J.; Epp, O.; Miki, K.; Huber, R.; Michel, H. *Nature* **1985**, *318*, 618. Allen, J. P.; Feher, G.; Yeates, T. O.; Komiya, H.; Rees, D. C. *Proc. Natl. Acad. Sci. U.S.A.* **1987**, *84*, 6162. Deisenhofer, J.; Michel, H. *Angew. Chem., Int. Ed. Engl.* **1989**, *28*, 829. Huber, R. *Angew. Chem., Int. Ed. Engl.* **1989**, *28*, 848. Hoff, A. J.; Deisenhofer, J. *Phys. Rep.* **1997**, *287*, 1. Zouni, A.; Witt, H.-T.; Kern, J.; Fromme, P.; Krauss, N.; Saenger, W.; Orth, P. *Nature* **2001**, *409*, 739.

(2) (a) McDermott, G.; Prince, S. M.; Freer, A. A.; Hawthornthwaite-Lawless, A. M.; Papiz, M. Z.; Cogdell, R. J.; Isaacs, N. W. *Nature* **1995**, *374*, 517. (b) Pullerits, T.; Sundström, V. *Acc. Chem. Res.* **1996**, *29*, 381. (c) Sundström, V.; Pullerits, T.; van Grondelle, R. *J. Phys. Chem. B* **1999**, *103*, 2327. (d) Sholes, G. D.; Fleming, G. R. *J. Phys. Chem. B* **2000**, *104*, 1854.

(3) Haser, R.; Pierrot, M.; Frey, M.; Payan, F.; Astier, J. P.; Bruschi, M.; Le Gall, J. *Nature* **1979**, *282*, 806. Iwata, S.; Ostermeier, C.; Ludwig, B.; Michel. H. *Nature* **1995**, *376*, 660. Tsukihara, T.; Aoyama, H.; Yamashita, E.; Tomizaka, T.; Yamaguchi, H.; Shinzawa-Itoh, K.; Nakashima, R.; Yaono, R.; Yoshikawa, S. *Science* **1995**, *269*, 1069. Moore, G. R. In *Protein Electron Transfer*; Bendall, D. S., Ed.; Bios Scientific Publishers: Oxford, UK, 1996; p 189 and references therein. Igarashi, N.; Moriyama, H.; Fujiwara, T.; Fukumori, Y.; Tanaka, N. *Nature Struct. Biol.* **1997**, *4*, 276.

(4) (a) Tabushi, I.; Kugimiya, S.-i.; Kinnaird, M. G.; Sasaki, T. *J. Am. Chem. Soc.* **1985**, *107*, 4192. (b) Osuka, A.; Maruyama, K. *J. Am. Chem. Soc.* **1988**, *110*, 4454. (c) Yang, S. I.; Lammi, R. K.; Seth, J.; Riggs, J. A.; Arai, T.; Kim, D.; Bocian, D. F.; Holten, D.; Lindsey, J. S. *J. Phys. Chem. B* **1998**, *102*, 9426.

(5) (a) Lin, V. S.-Y.; DiMagno, S. G.; Therien, M. J. *Science* **1994**, *264*, 1105. (b) Osuka, A.; Tanabe, N.; Nakajima, S.; Maruyama, K. *J. Chem. Soc., Perkin Trans. 2* **1996**, 199. (c) Arai, T.; Takei, K.; Nishino, N.; Fujimoto, T. *Chem. Commun.* **1996**, 2133. (d) Nakano, A.; Osuka, A.; Yamazaki, I.; Yamazaki, T.; Nishimura, Y. *Angew. Chem., Int. Ed.* **1998**, *37*, 3023. (e) Li, J.; Ambroise, A.; Yang, S. I.; Diers, J. R.; Seth, J.; Wack, C. R.; Bocian, D. F.; Holten, D.; Lindsey, J. S. *J. Am. Chem. Soc.* **1999**, *121*, 8927. (f) Sugiura, K.-i.; Tanaka, H.; Matsumoto, T.; Kawai, T.; Sakata, Y. *Chem. Lett.* **1999**, 1193 and references therein.

(6) Sanders, J. K. M. In *The Porphyrin Handbook*; Kadish, K. M., Smith, K. M., Guilard, R., Eds.; Academic Press: San Diego, 2000; Vol. 3, p 347 and references therein.

10.1021/jo030001k CCC: $25.00
Published on Web 06/06/2003

phyrin arrays by the combination of coordination bonds and hydrogen bonds.[8,9]

The natural multiple porphyrin systems are constructed via the self-assembling nature of both the proteins and the porphyrins. The natural porphyrins are linked by the polypeptides at their peripheral positions or coordinationally sandwiched by their central metals to afford the porphyrin−polypeptide hybrids, which are self-assembled to form the supramolecules.[2b] The porphyrin is a hydrophobic conjugated system, which is uncommon in biomolecules. The amino acids near the porphyrins tune their enzymatic and photochemical reactivities,[10] therefore, many groups have studied the conjugates of the porphyrins and the synthetic polypeptides.[11] The representative motif of the conjugates is a four α-helix bundle structure of the polypeptides built on one face of the porphyrin.[12] α-Helical polypeptides have been utilized to build porphyrin−polypeptide conjugates[13] because of their defined structures and their synthetic developments.[14] Recently, multiple porphyrin systems have been synthesized via a sophisticated design of the α-helical polypeptides which probably includes the hydrophobic interaction between the porphyrins.[15] However, these investigations showed that the α-helical polypeptides tend to take the monomeric structure or the isolated bundle structure with four or six polypeptide chains in a solution. This is probably because the hydrophobic and Coulombic interactions assemble the α-helical polypeptides, which are weaker than the multiple hydrogen bonds between the *β*-sheet polypeptides. Only in the seminatural systems, the further assembling of the porphyrin-linked polypeptides was attained with the assistance of the lipid molecules.[16]

The *β*-sheet structure of the polypeptides is another secondary structure that is found in some photosynthetic bacteria.[17] Although the synthetic chemistry of the soluble *β*-sheet polypeptides has been developed,[18,19] the *β*-sheet polypeptides still sometimes form the insoluble aggregates. However, its tendency to self-assemble is attractive in the modeling of the natural porphyrin clusters. In the amphiphilic *β*-sheet polypeptides with the alternative hydrophobic and hydrophilic amino acids sequences,[20] the hydrophobic amino acids are located on one face of the *β*-sheet and the hydrophilic amino acids on the other face. If the porphyrin is linked to the hydrophobic amino acids, the porphyrins will be assembled on the hydrophobic face, in which we can expect the $\pi-\pi$ interaction and the hydrophobic interaction between the porphyrins. These interactions will assemble the polypeptides besides the hydrogen bondings and stabilize the *β*-sheet structure. In this respect, it is interesting that the recently reported soluble *β*-sheet polypeptides contain the cluster of aromatic amino acids.[19d] Furthermore, it is worthy of note that the recently reported foldamers contain aromatic moieties.[21] If the hydrophobic interactions between the porphyrins gather the short polypeptide chains, the *β*-sheet structure may be soluble and stable with a few amino acid residues. In the *β*-sheet polypeptides linking the porphyrins, a number of porphyrins will be arranged on the hydrophobic face of the *β*-sheet because of its polymeric feature, which will be a new candidate to model the natural porphyrin assembly. Besides these potentials, the *β*-sheet polypeptides have rarely been studied for the construction of supramolecular porphyrins.[22] Thus, we have

(7) Biemans, H. A. M.; Rowan, A. E.; Verhoeven, A.; Vanoppen, P.; Latterini, L.; Foekema, J.; Schenning, A. P. H. J.; Meijer, E. W.; de Schryver, F. C.; Nolte, R. J. M. *J. Am. Chem. Soc.* **1998**, *120*, 11054. Maruo, N.; Uchiyama, M.; Kato, T.; Arai, T.; Akisada, H.; Nishino, N. *Chem. Commun.* **1999**, 2057 and references therein.

(8) Chambron, J.-C.; Heitz, V.; Sauvage, J.-P. In *The Porphyrin Handbook*; Kadish, K. M., Smith, K. M., Guilard, R., Eds.; Academic Press: San Diego, CA, 2000; Vol. 6, p 1 and references therein.

(9) Kobuke, Y.; Miyaji, H. *J. Am. Chem. Soc.* **1994**, *116*, 4111. Sessler, J. L.; Wang, B.; Harriman, A. *J. Am. Chem. Soc.* **1995**, *117*, 704. Lahiri, J.; Fate, G. D.; Ungashe, S. B.; Groves, J. T. *J. Am. Chem. Soc.* **1996**, *118*, 2347. Feiters, M. C.; Fyfe, M. C. T.; Martínez-Díaz, M.-V.; Menzer, S.; Nolte, R. J. M.; Stoddart, J. F.; van Kan, P. J. M.; Williams, D. J. *J. Am. Chem. Soc.* **1997**, *119*, 8119. Fan, J.; Whiteford, J. A.; Olenyuk, B.; Levin, M. D.; Stang, P. J.; Fleischer, E. B. *J. Am. Chem. Soc.* **1999**, *121*, 2741. Solladié, N.; Chambron, J.-C.; Sauvage, J.-P. *J. Am. Chem. Soc.* **1999**, *121*, 3684. Taylor, P. N.; Anderson, H. L. *J. Am. Chem. Soc.* **1999**, *121*, 11538.

(10) Lu, Y.; Berry, S. M.; Pfister, T. D. *Chem. Rev.* **2001**, *101*, 3047 and references therein.

(11) Lombardi, A.; Nastri, F.; Pavone, V. *Chem. Rev.* **2001**, *101*, 3165 and references therein.

(12) (a) Sasaki, T.; Kaiser, E. T. *J. Am. Chem. Soc.* **1989**, *111*, 380. (b) Åkerfeldt, K. S.; Kim, R. M.; Camac, D.; Groves, J. T.; Lear, J. D.; DeGrado, W. F. *J. Am. Chem. Soc.* **1992**, *114*, 9656. (c) Choma, C. T.; Kaestle, K.; Åkerfeldt, K. S.; Kim, R. M.; Groves, J. T.; DeGrado, W. F. *Tetrahedron Lett.* **1994**, *35*, 6191. (d) Arai, T.; Kobata, K.; Mihara, H.; Fujimoto, T.; Nishino, N. *Bull. Chem. Soc. Jpn.* **1995**, *68*, 1989.

(13) Pispisa, B.; Palleschi, A.; Venanzi, M.; Zanotti, G. *J. Phys. Chem.* **1996**, *100*, 6835. Nastri, F.; Lombardi, A.; Morelli, G.; Maglio, O.; D'Auria, G.; Pedone, C.; Pavone, V. *Chem. Eur. J.* **1997**, *3*, 340. Huffman, D. L.; Rosenblatt, M. M.; Suslick, K. S. *J. Am. Chem. Soc.* **1998**, *120*, 6183. Geier, G. R., III; Sasaki, T. *Tetrahedron* **1999**, *55*, 1859. Liu, D.; Williamson, D. A.; Kennedy, M. L.; Williams, T. D.; Morton, M. M.; Benson, D. R. *J. Am. Chem. Soc.* **1999**, *121*, 11798. Arai, T.; Tsukuni, A.; Kawazu, K.; Aoi, H.; Hamada, T.; Nishino, N. *J. Chem. Soc., Perkin Trans. 2* **2000**, 1381.

(14) (a) Voyer, N. In *Topics in Current Chemistry, 184*; Schmidtchen, F. P., Ed.; Springer-Verlag: Berlin, 1997; p 1. (b) Hill, R. B.; Raleigh, D. P.; Lombardi, A.; DeGrado, W. F. *Acc. Chem. Res.* **2000**, *33*, 745. (c) Baltzer, L.; Nilsson, H.; Nilsson, J. *Chem. Rev.* **2001**, *101*, 3153.

(15) (a) Rau, H. K.; Haehnel, W. *J. Am. Chem. Soc.* **1998**, *120*, 468. (b) Sharp, R. E.; Diers, J. R.; Bocian, D. F.; Dutton, P. L. *J. Am. Chem. Soc.* **1998**, *120*, 7103. (c) Sharp, R. E.; Moser, C. C.; Rabanal, F.; Dutton, P. L. *Proc. Natl. Acad. Sci. U.S.A.* **1998**, *95*, 10465. (d) Ushiyama, M.; Yoshino, A.; Yamamura, T.; Shida, Y.; Arisaka, F. *Bull. Chem. Soc. Jpn.* **1999**, *72*, 1351. (e) Shifman, J. M.; Gibney, B. R.; Sharp, R. E.; Dutton, P. L. *Biochemistry* **2000**, *39*, 14813. (f) Tomizaki, K.-y.; Murata, T.; Kaneko, K.; Miike, A.; Nishino, N. *J. Chem. Soc., Perkin Trans. 2* **2000**, 1067. (g) Sakamoto, M.; Ueno, A.; Mihara, H. *Chem. Eur. J.* **2001**, *7*, 2449.

(16) Nango, M.; Kashiwada, A.; Watanabe, H.; Yamada, S.; Yamada, T.; Ogawa, M.; Tanaka, T.; Iida, K. *Chem. Lett.* **2002**, 312.

(17) Tronrud, D. E.; Schmid, M. F.; Matthews, B. W. *J. Mol. Biol.* **1986**, *188*, 443.

(18) For review, see: Gellman, S. H. *Curr. Opin. Chem. Biol.* **1998**, *2*, 717. Lacroix, E.; Kortemme, T.; Lopez de la Paz, M.; Serrano, L. *Curr. Opin. Struct. Biol.* **1999**, *9*, 487. Searle, M. S. *J. Chem. Soc., Perkin Trans. 2* **2001**, 1011. See also refs 14a and 14c.

(19) (a) Ono, S.; Kameda, N.; Yoshimura, T.; Shimasaki, C.; Tsukurimichi, E.; Mihara, H.; Nishino, N. *Chem. Lett.* **1995**, 965. (b) Aggeli, A.; Bell, M.; Boden, N.; Keen, J. N.; Knowles, P. F.; McLeish, T. C. B.; Pitkeathly, M.; Radford, S. E. *Nature* **1997**, *386*, 259. (c) Takahashi, Y.; Yamashita, T.; Ueno, A.; Mihara, H. *Tetrahedron* **2000**, *56*, 7011. (d) Griffiths-Jones, S. R.; Searle, M. S. *J. Am. Chem. Soc.* **2000**, *122*, 8350. (e) Mezo, A. R.; Ottesen, J. J.; Imperiali, B. *J. Am. Chem. Soc.* **2001**, *123*, 1002. (f) Nowick, J. S.; Cary, J. M.; Tsai, J. H. *J. Am. Chem. Soc.* **2001**, *123*, 5176. (g) Kaul, R.; Angeles, A. R.; Jäger, M.; Powers, E. T.; Kelly, J. W. *J. Am. Chem. Soc.* **2001**, *123*, 5206.

(20) Osterman, D.; Mora, R.; Kézdy, F. J.; Kaiser, E. T.; Meredith. S. C. *J. Am. Chem. Soc.* **1984**, *106*, 6845. Mutter, M.; Hersperger, R. *Angew. Chem., Int. Ed. Engl.* **1990**, *29*, 185. Dado, G. P.; Gellman. S. H. *J. Am. Chem. Soc.* **1993**, *115*, 12609.

(21) Lokey, R. S.; Iverson, B. L. *Nature* **1995**, *375*, 303. Nelson, J. C.; Saven, J. G.; Moore, J. S.; Wolynes, P. G. *Science* **1997**, *277*, 1793. Gin, M. S.; Yokozawa, T.; Prince, R. B.; Moore, J. S. *J. Am. Chem. Soc.* **1999**, *121*, 2643. Prince, R. B.; Brunsveld, L.; Meijer, E. W.; Moore, J. S. *Angew. Chem., Intl. Ed.* **2000**, *39*, 228. Zych, A. J.; Iverson, B. L. *J. Am. Chem. Soc.* **2000**, *122*, 8898.

(22) Arai, T.; Maruo, N.; Sumida, Y.; Korosue, C.; Nishino, N. *Chem. Commun.* **1999**, 1503. Arai, T.; Araki, K.; Fukuma, K.; Nakashima, T.; Kato, T.; Nishino, N. *Chem. Lett.* **2002**, 1110.

SCHEME 1

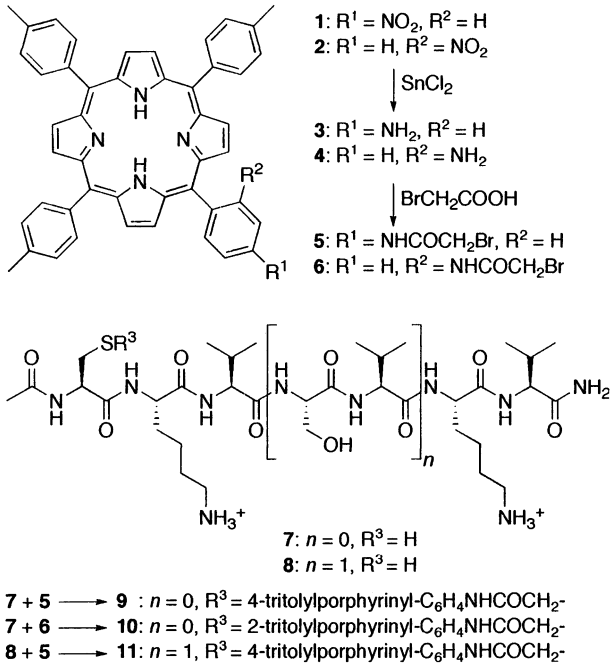

synthesized and briefly communicated the porphyrins conjugated with the acyclic polypeptides which could take the β-sheet structure.[23] Here we report the full investigation of the interactions between porphyrins to explain the spectroscopic results, together with the chromatographic and ^{1}H NMR studies, and also show a new methodology to assemble the porphyrins by conjugation with the acyclic β-sheet polypeptides.

Results and Discussion

Syntheses of Porphyrins Linking Acyclic Peptides. Porphyrins **1** and **2** with a single nitro group were synthesized via a modified Lindsey's method ([pyrrole] = 0.20 M and [BF_3OEt_2] = 60 mM) and isolated via chromatography (Scheme 1).[24] Using high concentrations for the reactants and acid, the porphyrins were produced on a subgram scale although the yields were not high (4−5%). The *p*-tolyl groups were introduced to increase the solubility of the porphyrins and to clarify the ^{1}H NMR analyses. The nitro groups of **1** and **2** were reduced by $SnCl_2$[24c,25] to afford the aminoporphyrins **3** and **4**, then bromoacetic acid was condensed with EDC HCl[26,27] to afford the bromoacetamido-linked porphyrins **5** and **6** (Scheme 1).

The amphiphilic pentapeptide **7** and heptapeptide **8** with alternative hydrophilic/hydrophobic sequences were adopted, while considering the peptide length (one amino acid residue ≈0.34 nm) and the porphyrin radius (0.69 nm between *meso*-carbons and 1.83 nm between tolyl-*Me* carbons). Val was employed as the hydrophilic amino acid because of its high tendency to form the β-sheet structure.[28] Lys was chosen as the hydrophilic amino acid from its solubility; however, a Ser residue was used in **8** to equalize the net peptide charges. The N- and C-termini were capped by Ac and NH_2, respectively. Peptides **7** and **8** were manually synthesized on the Rink-amide resin[29] with a standard Fmoc-chemistry, using PyBOP−HOBt[30] as the condensation reagents. After the cleavage of the peptides from the resins, the peptides were purified by reversed phase HPLC and isolated as the hydrated TFA salts, in which their Ellman's determinations[31] showed the ca. 50% contents of the free peptides (see the Experimental Section).

The bromoacetamido-linked porphyrins (**5** and **6**) and Cys-peptides (**7** and **8**) were coupled in DMF in the presence of excess base. The reactions were monitored by HPLC analyses, in which some gels or precipitates were formed in the reaction mixtures. The peptides (**7** and **8**) did not contain any oxidized S−S dimers (see the Experimental Section), therefore, no reductant (such as 1,2-ethanedithiol) was added in contrast to our previous system.[15f] Thus, the porphyrins linking acyclic peptides **9**, **10**, and **11** were obtained in favorable yields (68, 91, and 78%, respectively) after HPLC purification. These porphyrin−peptide conjugates and also the intermediates were characterized by ^{1}H NMR (1D and 2D ^{1}H−^{1}H COSY), MS/HIMS, and the amino acid analyses. In the MALDI-TOF-MS spectra, **9** showed not only the $[M + H]^+$ signal of *m*/*z* 1330 but also the signals of dimeric **9** at *m*/*z* 2691 (calcd for 2M + Na, 2680) and trimeric **9** at *m*/*z* 4021 (calcd for 3M + Na, 4009). MALDI-TOF-MS also showed the dimeric **11** at *m*/*z* 3062 (calcd for 2M + Na, 3053) as well as the monomer. These signals of dimer and trimer implied the molecular assembling of **9** and **11**.

In the ^{1}H NMR spectrum of the conjugate **10** linking peptide at the *o*-phenyl position, some of the peptide signals were high-field shifted compared to the conjugates **9** linking the peptides at the *p*-phenyl positions (Table 1). The upfield shifts of **10** compared to **9** were 0.7−0.8 ppm for Cys-CβH, ∼0.5 for Cys-CαH and Cys-NH, and ∼0.3 for Ac and one Lys-αH. The other signals, such as Val-γH, showed ∼0.1 ppm upfield shifts. These results showed that the porphyrin ring existed near the polypeptide chains in **10**.

(23) Arai, T.; Inudo, M.; Ishimatsu, T.; Sasaki, T.; Kato, T.; Nishino, N. *Chem. Lett.* **2001**, 1240.

(24) (a) Nishino, N.; Sakamoto, T.; Kiyota, H.; Mihara, H.; Yanai, T.; Fujimoto, T. *Chem. Lett.* **1993**, 279. (b) Lindsey, J. S.; MacCram, K. A.; Tyhonas, J. S.; Chuang, Y.-Y. *J. Org. Chem.* **1994**, *59*, 579. (c) Sol, V.; Blais, J. C.; Carré, V.; Granet, R.; Guilloton, M.; Spiro, M.; Krausz, P. *J. Org. Chem.* **1999**, *64*, 4431.

(25) Collman, J. P.; Gagne, R. R.; Reed, C. A.; Halbert, T. R.; Lang, G.; Robinson, W. T. *J. Am. Chem. Soc.* **1975**, *97*, 1427.

(26) Dawson, P. E.; Kent, S. B. H. *J. Am. Chem. Soc.* **1993**, *115*, 7263. Robey, F. A. In *Methods in Molecular Biology*; Peptide Synthesis Protocols, No. 35; Pennington, M. W., Dunn, B. M., Eds.; Humana Press: Totowa, NJ, 1994; p 73. Geier, G. R., III; Sasaki, T. *Tetrahedron Lett.* **1997**, *38*, 3821. See also refs 12c and 15f.

(27) Abbreviations used are according to IUPAC-IUB commission: *Eur. J. Biochem.* **1984**, *138*, 9. Other abbreviations: bis-tris, 2,2-bis-(hydroxymethyl)-2, 2′,2″-nitrilotriethanol; bis-tris propane, 1,3-bis(tris-(hydroxymethyl)methylamino)propane; CAPSO, 3-cyclohexylamino-2-hydroxy-1-propanesulfonic acid; EDC, 1-(3-dimethylaminopropyl)-3-ethylcarbodiimide; Fmoc, 9-fluorenylmethoxycarbonyl; HEPPSO, 2-hydroxy-3-(4-(2-hydroxyethyl)-1-piperazinyl)propanesulfonic acid; HIMS, high-resolution mass spectroscopy; HOBt, 1-hydroxybenzotriazole; PyBOP, benzotriazole-1-yloxytrispyrrolidinophosphonium hexafluorophosphate; Rink-amide resin, 4-(2′,4′-dimethoxyphenyl-α-aminomethyl)phenoxy resin; SEC, size exclusion chromatography; TFE, 2,2,2-trifluoroethanol; tris, tris(hydroxymethyl)aminomethane.

(28) Chou, P. Y.; Fasman, G. D. *Adv. Enzymol.* **1978**, *47*, 45.

(29) Rink, H. *Tetrahedron Lett.* **1987**, *28*, 3787.

(30) Coste, J.; Le-Nguyen, D.; Castro, B. *Tetrahedron Lett.* **1990**, *31*, 205.

(31) Grassetti, D. R.; Murray, J. F., Jr. *Arch. Biochem. Biophys.* **1967**, *119*, 41.

TABLE 1. Selected ^{1}H NMR Chemical Shifts (δ/ppm) of Petpides and Porphyrins[a]

	Val-CγH	Ac	Cys-CβH	Cys-CαH	Lys-αNH	Cys-NH
7	0.81, 0.83	1.86	2.67, 2.74	4.36	8.04, 8.18	8.09
9	0.80, 0.84	1.90	2.92, 3.09	4.57	8.08, 8.29	8.33
10	0.67, 0.77	1.57	2.11, 2.39	4.07	7.90, 7.96	7.84
11	0.82	1.93	2.93, 3.10	4.60	8.01, 8.27	8.32

[a] Measured in DMSO-d_6 at 298 K.

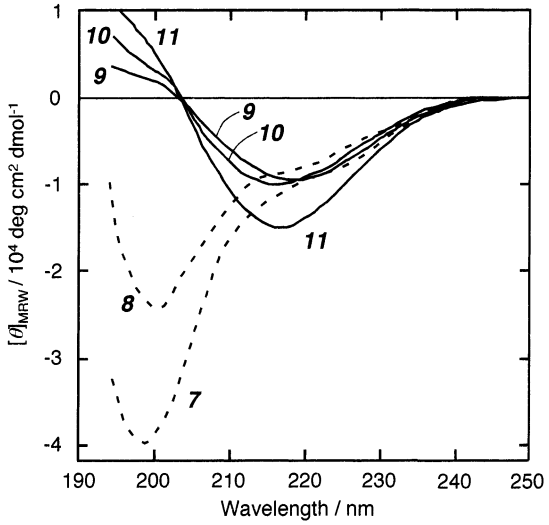

FIGURE 1. CD spectra (amide region) of **7**, **8**, **9**, **10**, and **11** (40 μM) in pH 9.0 buffer solution with 20% TFE (v/v).

CD Spectra in the Amide Region. Figure 1 shows the CD spectra of peptides **7** and **8** and porphyrin-linked peptides **9**−**11** (40 μM, amide region) in the pH 9.0 buffer solution (10 mM bis-tris propane) with 20% TFE (v/v). Peptides **7** and **8** showed negative Cotton effects at around 200 nm (**7**; $[\theta]_{MRW} = -39\,800$ deg cm^2 dmol^{-1} at 199 nm, **8**; $[\theta]_{MRW} = -24\,600$ at 201 nm, $[\theta]_{MRW}$/deg cm^2 dmol^{-1} = 3300 × $\Delta\epsilon$/M^{-1} cm^{-1} per mean residue weight, i.e., 5 for **7** and 7 for **8**) with shoulder peaks at around 222 nm. These CD spectra indicated that these peptides were of a random structure in this solvent (the CD spectrum of the random coil peptide is, for instance, $[\theta]_{MRW} = -41\,900$ deg cm^2 dmol^{-1} at 197 nm for poly(Lys) at pH 7).[32,33] Compared with the reported amphiphilic β-sheet polypeptides (13−18 amino acid residues),[20] penta- and heptapeptides are too short to take the stable β-sheet structure. However, the peptide frameworks of **9**−**11** showed negative Cotton effects at around 217 nm (**9**; $[\theta]_{MRW} = -9\,400$ at 219 nm, **10**; $[\theta]_{MRW} = -9\,900$ at 216 nm, **11**; $[\theta]_{MRW} = -14\,700$ at 217 nm), which is a characteristic of the β-sheet peptides.[33] The CD spectra of the β-sheet peptides differs significantly depending on the amino acid residues, solvents, and their aggregation properties, varying from $[\theta]_{MRW}$ of −9 000 to −18 400 at 217 nm.[32,33c,34] The other Cotton effect characteristic of the β-sheet peptide at around 195 nm was not detected in our solvent. Moreover, we cannot exclude the possibility that the porphyrin rings in **9**−**11** might show some Cotton effect in the amide-region CD spectra. Besides these ambiguities, these CD spectra of **9**−**11** suggested that the peptide frameworks linking the porphyrins were of the β-sheet structure, in contrast to the random structure of the free peptides, **7** and **8**. The hydrophobic porphyrins attached at Cys induced the β-sheet structure, probably via a hydrophobic interaction between porphyrins (see below). The large $[\theta]_{217}$ value of **11** compared to **9** and **10** implied that its heptapeptide structure formed a stable β-structure.

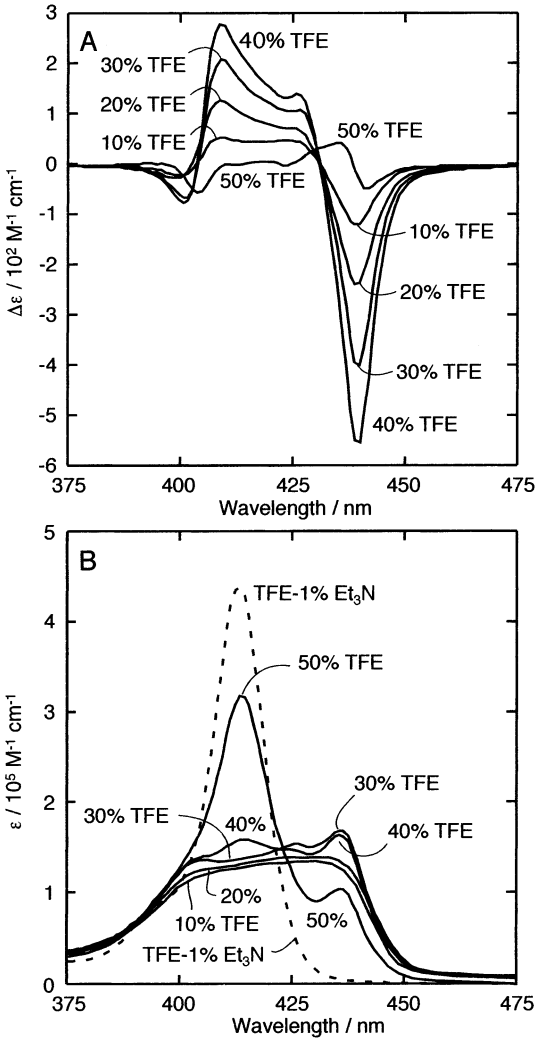

FIGURE 2. (A) CD and (B) UV/vis spectra (Soret region) of **9** (40 μM) in pH 9.0 buffer solution with 10%, 20%, 30%, 40%, and 50% TFE (v/v), and in TFE−1% Et$_3$N (only in B).

CD and UV/vis Spectra of 9 in the Porphyrin Soret Region. Figure 2A shows the CD spectra of **9** (40 μM in the pH 9.0 buffer solution containing TFE), where strong Cotton effects appeared in the porphyrin Soret band region. The Cotton effects were the strongest in the pH 9.0 buffer solution with 40% TFE among the various

(32) Greenfield, N.; Fasman, G. D. *Biochemistry* **1969**, *8*, 4108.

(33) (a) Woody, R. W. In *Circular Dichroism: Principles and Applications*; Nakanishi, K., Berova, N., Woody, R. W., Eds.; VCH: New York, 1994; p 473. (b) Venyaminov, S. Y.; Yang, J. T. In *Circular Dichroism and the Conformational Analysis of Biomolecules*; Fasman, G. D., Ed.; Plenum: New York, 1996; p 69. (c) Tilstra, L.; Mattice, W. L. In *Circular Dichroism and the Conformational Analysis of Biomolecules*; Fasman, G. D., Ed.; Plenum: New York, 1996; p 261.

(34) Sarkar, P. K.; Doty, P. *Proc. Natl. Acad. Sci. U.S.A.* **1966**, *55*, 981.

examined solvent systems (see below) with $\Delta\epsilon_{440} = -559$ M^{-1} cm^{-1}, $\Delta\epsilon_{426} = 139$ M^{-1} cm^{-1}, $\Delta\epsilon_{409} = 279$ M^{-1} cm^{-1}, and $\Delta\epsilon_{402} = -73.9$ M^{-1} cm^{-1}. Such strong Cotton effects of $\Delta\epsilon > 10^2$ M^{-1} cm^{-1} were assigned to the exciton coupled Cotton effects between the porphyrins.[35−39] The monomeric porphyrin in the protein shows a weak Cotton effect induced by the amino acids, for instance, the Cotton effects of the hemes in the cytochromes are $\Delta\epsilon < 10^2$ M^{-1} cm^{-1},[40,41] which are usually with a single band. In contrast, the exciton coupled Cotton effects are derived from two or more porphyrin chromophores, generally showing two strong CD bands with inverse signs such as −/+ or +/−. Thus, the CD spectra of **9** showed that the porphyrins were located nearby, like the cluster of the aromatic amino acids in the designed β-sheet polypeptides,[19d] while the hydrophobic porphyrins may arrange on one face (the hydrophobic face) of the amphiphilic β-sheet.

The Cotton effects of **9** increased in the order of pH 9.0 with 10% TFE < 20% TFE < 30% TFE < 40% TFE, however, they broke down in 50% TFE (Figure 2A). In the hydrophobic solvent containing a large amount of TFE, the hydrogen bondings of the β-sheet structure were stabilized[42] but the hydrophobic interaction between the porphyrins was weakened. No CD signals appeared in the porphyrin region in TFE or in TFE−1% Et_3N. Thus, the hydrophobic interaction between the porphyrins was important in the assembling of **9**.

The strength of the Cotton effects of **9** was in the order of pH 8.0 with 20% TFE < pH 9.0 with 20% TFE > pH 10.0 with 20% TFE (Figure 3). At pH 8.0, the Coulombic repulsion of the protonated Lys side chains inhibited the assembling of **9**. At pH 10.0, some of the Lys side chains were deprotonated and the amphiphilic structure of **9** would be disordered. The fact that the pK_a value of Lys-ϵ-NH_3^+ is 10.54[43] supported this interpretation. The internal charge repulsion model may be important to interpret these pH effects,[44] which will be carried out in the future.

The UV/vis spectra gave further information as to the assembling of **9** (Figure 2B). In TFE−1% Et_3N (note, **9** was isolated as the TFA salts), **9** showed a sharp absorption at 413 nm with a molar absoptivity ϵ of 443 000 M^{-1} cm^{-1}. In this solvent, the molar absoptivity of tetraphenylporphyrin ($\epsilon_{410} = 468\,000$ M^{-1} cm^{-1}) was similar to the reported value ($\epsilon_{419} = 470\,000$ M^{-1} cm^{-1} in benzene).[45] In pH 9.0 buffer solution with 50% TFE, **9** (40 μM) showed two absorptions at 436 and 414 nm, where the absorption at 414 nm was of the monomeric porphyrin and the peak at 436 nm was from the assembled porphyrins (see below).[46] In 30% TFE, **9** showed multiple absorptions at 436, 423, 414, and 402 nm, which would arise from the multiple interactions between porphyrins, as in the case of the CD spectra. The absorption at 414 nm almost disappeared in 20% TFE, which was judged by the second derivatives of the spectrum, and three absorptions appeared at 436, 424, and 403 nm. The absorptions of **9** in the assembled structure were generally broadened and small (Figure 2B), probably because many kinds of porphyrins existed in the polymeric β-sheet structure.[37d] It is interesting that **9** showed a slight Cotton effect in pH 9.0 buffer solution with 50% TFE, although the UV/vis spectra in the same solvent clearly showed the absorption of the aggregated species. No CD/UV spectral change was observed in the concentrated (200 μM) and low-temperature (273 K) solutions in this solvent. Further investigation on the aggregation in pH 9.0 buffer solution with 50% TFE will be carried out with use of fluorescence spectroscopy. The addition of the buffer solution to **9** in TFE−1% Et_3N changed the UV/vis spectra slightly (~3 nm) in the Q-band region (500−700 nm); however, no CD bands appeared in this region probably because of the small molar absorptivity for these absorptions.

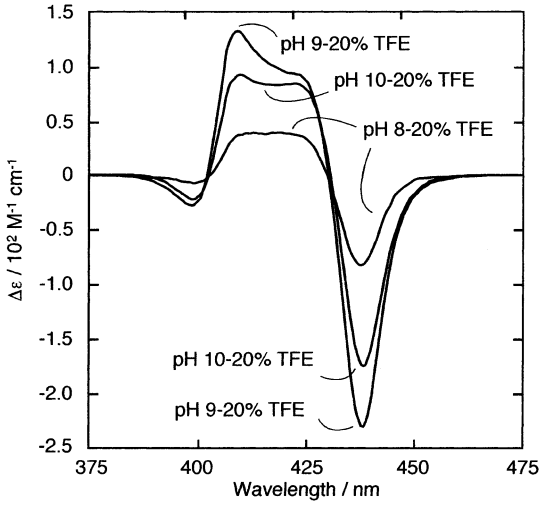

FIGURE 3. CD spectra (Soret region) of **9** (40 μM) in pH 8.0, 9.0, and 10.0 buffer solution with 20% TFE (v/v).

Orientation of Porphyrins in the Assembled Structure of 9. The Cotton effects of **9** (Figure 2A) were distorted from the general exciton coupled Cotton effects, which consist of two bands of inverse signs (−/+ or +/−).[35−39] These distorted Cotton effects of **9** could be the

(35) Berova, N.; Nakanishi, K. In *Circular Dichroism: Principles and Applications*, 2nd ed.; Berova, N., Nakanishi, K., Woody, R. W., Eds.; John Wiley and Sons: New York, 2000; p 337.
(36) Huang, X.; Nakanishi, K.; Berova, N. *Chirality* **2000**, *12*, 237.
(37) (a) Crossley, M. J.; Mackay, L. G.; Try, A. C. *J. Chem. Soc., Chem. Commun.* **1995**, 1925. (b) Takeuchi, M.; Imada, T.; Shinkai, S. *J. Am. Chem. Soc.* **1996**, *118*, 10658. (c) Hayashi, T.; Nonoguchi, M.; Aya, T.; Ogoshi, H. *Tetrahedron Lett.* **1997**, *38*, 1603. (d) Huang, X.; Borhan, B.; Berova, N.; Nakanishi, K. *J. Indian Chem. Soc.* **1998**, *75*, 725. (e) Huang, X.; Borhan, B.; Rickman, B. H.; Nakanishi, K.; Berova, N. *Chem. Eur. J.* **2000**, *6*, 216.
(38) Borovkov, V. V.; Lintuluoto, J. M.; Fujiki, M.; Inoue, Y. *J. Am. Chem. Soc.* **2000**, *122*, 4403. Borovkov, V. V.; Lintuluoto, J. M.; Inoue, Y. *J. Am. Chem. Soc.* **2001**, *123*, 2979. See also refs 5c, 15f, and 22.
(39) Liang, K.; Farahat, M. S.; Perlstein, J.; Law, K.-Y.; Whitten, D. G. *J. Am. Chem. Soc.* **1997**, *119*, 830. Lu, L.; Lachicotte, R. J.; Penner, T. L.; Perlstein, J.; Whitten, D. G. *J. Am. Chem. Soc.* **1999**, *121*, 8146. Zeena, S.; Thomas, K. G. *J. Am. Chem. Soc.* **2001**, *123*, 7859.
(40) Myer, Y. P.; Pande, A. In *The Porphyrins*; Dolphin, D., Ed.; Academic Press: New York, 1978; Vol. III, p 271.
(41) Hsu, M.-C.; Woody, R. W. *J. Am. Chem. Soc.* **1971**, *93*, 3515.
(42) Rohl, C. A.; Chakrabartty, A.; Baldwin, R. L. *Protein Sci.* **1996**, *5*, 2623. Arai, T.; Imachi, T.; Kato, T.; Nishino, N. *Bull. Chem. Soc. Jpn.* **2000**, *73*, 439.
(43) Dawson, R. M. C.; Elliot, D. C.; Elliot, W. H.; Jones, K. M. In *Data for Biochemical Research*, 3rd ed.; Oxford University Press: Oxford, UK, 1986; p 23.
(44) Baumeister, B.; Som, A.; Das, G.; Sakai. N.; Vilbois, F.; Gerard, D.; Shahi, S. P.; Matile, S. *Helv. Chim. Acta* **2002**, *85*, 2740 and references therein.
(45) Kim, J. B.; Leonard, J. J.; Longo, F. R. *J. Am. Chem. Soc.* **1972**, *94*, 3986.
(46) Ohno, O.; Kaizu, Y.; Kobayashi, H. *J. Chem. Phys.* **1993**, *99*, 4128.

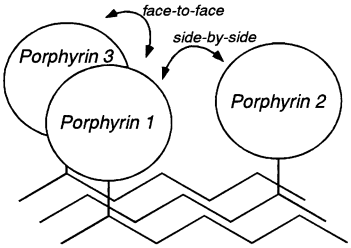

FIGURE 4. Illustration for the trimeric **9** depicting the face-to-face orientation between *porphyrin 1* and *porphyrin 3*, and depicting the side-by-side orientation between *porphyrin 1* and *porphyrin 2*.

sum of two or more sets of Cotton effects, for instance, 440(−)/426(+) and 409(+)/402(−), though these signals did not completely match the UV/vis absorptions at 436, 424, and 403 nm. The appearance of two sets of Cotton effects and multiple UV/vis absorptions suggested that more than two kinds of exciton couplings occurred in the assembled structure of **9**. If more than three molecules of **9** were involved in the β-sheet structure, at least two porphyrin−porphyrin interactions occur (Figure 4). The porphyrins of the first (*porphyrin 1*) and the second (*porphyrin 2*) chains are of the side-by-side orientation. The porphyrins of the first (*porphyrin 1*) and the third (*porphyrin 3*) chains are of the face-to-face orientation.

From Kasha's theory about exciton coupling and the orientation of the transition moment in porphyrins, the side-by-side interaction of the chromophores produces the longwave shift in the absorption spectra and the face-to-face interaction produces the shortwave shift,[47] although the details of the interaction between the porphyrins are not yet clear.[48] The longwave shifted absorption derived from the aggregated porphyrins is often observed in water-soluble porphyrins[49] and the dimeric porphyrins in a side-by-side fashion.[4b,22] The shortwave shifted absorptions are also observed in the dimeric porphyrins in a face-to-face fashion.[4b,50] These interactions between porphyrins explain the two sets of Cotton effects and the multiple UV/vis absorptions of **9**. The two porphyrins (*porphyrins 1* and *2*) are in the side-by-side orientation, in which the porphyrin excitons are (in the HNC_6H_4−porphyrin−tolyl axis) somewhat twisted by the chiral amino acids. The negative band at 440 nm and the positive band at 426 nm in the CD spectra of **9** (Figure 2A) arise from the exciton coupling between *porphyrin 1* and *porphyrin 2*. The positive band at 409 nm and the negative band at 402 nm in the CD spectra of **9** arise from the exciton coupling between *porphyrins 1* and *3*, in which the two excitons are in the face-to-face orientation. It may be noted here that the ^{1}H NMR analysis of the conjugate in such dilute solution is difficult (see below for the ^{1}H NMR of the concentrated solution).

(47) Kasha, M.; Rawls, H. R.; El-Bayoumi, M. A. *Pure Appl. Chem.* **1965**, *11*, 371.
(48) Hunter, C. In *From Simplicity to Complexity in Chemistry and Beyond*; Müller, A., Dress, A., Vögel, F., Eds.; Vieweg: Braunschweig, Germany, 1996; p 113.
(49) Hambright, P. In *The Porphyrin Handbook*; Kadish, K. M., Smith, K. M., Guilard, R., Eds.; Academic Press: San Diego, CA, 2000; Vol. 3, p 129.
(50) Dubowchik, G. M.; Hamilton, A. D. *J. Chem. Soc., Chem. Commun.* **1986**, 665.

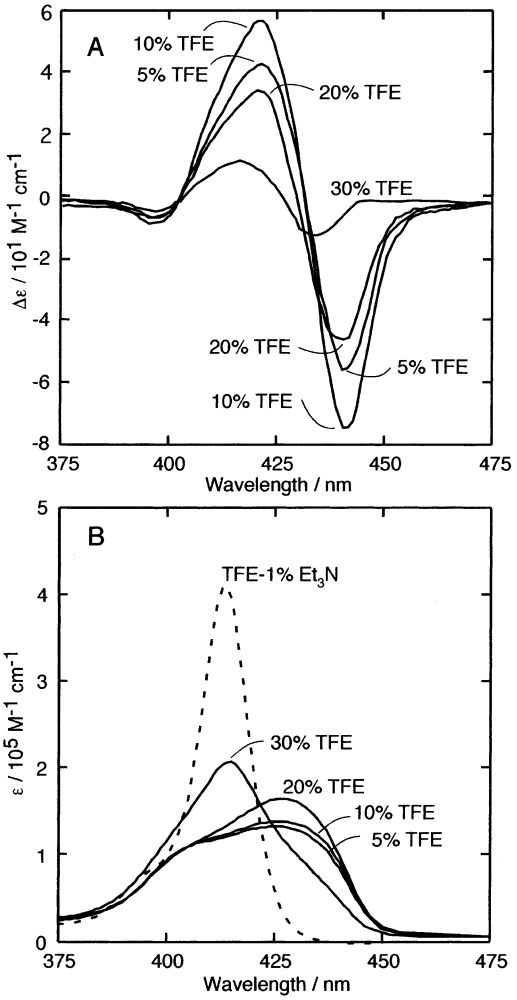

FIGURE 5. (A) CD and (B) UV/vis spectra (Soret region) of **10** (40 μM) in pH 9.0 buffer solution with 5%, 10%, 20%, 30% TFE (v/v), and in TFE−1% Et_3N (only in B).

CD and UV/vis Study of 10. The porphyrin linking the pentapeptide at the *o*-phenyl position, **10**, showed weak Cotton effects in the Soret region (Figure 5A). The Cotton effects of **10** were weak and simple compared to those of **9**, almost assignable to be negative chirality of the −/+ sign. The Cotton effects were strongest in the pH 9.0 buffer solution with 10% TFE, with $\Delta\epsilon_{439} = -77.9$ M^{-1} cm^{-1}, $\Delta\epsilon_{420} = 54.2$ M^{-1} cm^{-1}, and $\Delta\epsilon_{396} = -11.6$ M^{-1} cm^{-1}. The strength of the Cotton effects was in the order of pH 9.0 with 5% TFE < pH 9.0 with 10% TFE > pH 9.0 with 20% TFE > pH 9.0 with 30% TFE (Figure 5A). The aggregate of **10** was unstable and thus could be broken with the addition of 20% TFE, while that of **9** was stable in up to 40% TFE (Figure 2A). It is not yet clear why the Cotton effect of **10** was weak in pH 9.0 with 5% TFE, while the strength of the Cotton effects was in the order of pH 8.0 with 20% TFE < pH 9.0 with 20% TFE > pH 10.0 with 20% TFE (not shown), which was similar in the case of **9**. The absorption of **10** (414 nm in TFE−1% Et_3N) broadened with the addition of the pH 9.0 buffer solution and shifted to 427 nm, and shoulder peaks appeared at 403 and 437 nm (Figure 5B). However, these UV/vis spectral changes were not clear as in the case of **9**.

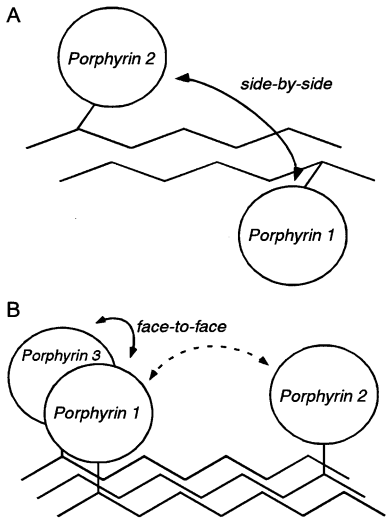

FIGURE 6. (A) Illustration for the dimeric **10** with side-by-side orientation between *porphyrin 1* and *porphyrin 2*. (B) Illustration for the trimeric **11** with face-to-face orientation-between *porphyrin 1* and *porphyrin 3*.

These facts showed that the assembled structure of **10** was more unstable than that of **9**, because of the steric repulsion of the porphyrins attached at the *o*-phenyl position as is illustrated in Figure 6A. Probably the porphyrins located exterior of the dimeric β-sheet peptides and disturbed the polymer formation. The two porphyrins in the dimeric **10** were located apart, which could not stabilize the aggregate without the face-to-face interaction and caused the weak Cotton effect. The absence of the face-to-face interaction was also suggested by the CD spectra, only showing the exciton coupled Cotton effect in the longwave shifted region. In contrast to the aggregate of **9** showing the Cotton effect in the longwave shifted region from the *porphyrins 1* and *2* and the Cotton effect in the shortwave shifted region from *porphyrins 1* and *3*, **10** only showed the Cotton effect in the longwave shifted region because of its dimeric structure.

CD and UV/vis Study of 11. The porphyrin with a heptapeptide at the *p*-phenyl position, **11**, also showed weak Cotton effects (Figure 7A). The Cotton effects were strongest in the pH 9.0 buffer solution with 30% TFE, with $\Delta\epsilon_{443} = -9.68\ M^{-1}\ cm^{-1}$, $\Delta\epsilon_{426} = 25.2\ M^{-1}\ cm^{-1}$, $\Delta\epsilon_{408} = -29.7\ M^{-1}\ cm^{-1}$, and $\Delta\epsilon_{392} = 8.44\ M^{-1}\ cm^{-1}$, but were weak in pH 9.0 with 20% TFE or in pH 9.0 with 40% TFE. The Cotton effects were the strongest in the pH 9.0 buffer solution with 30% TFE and were weak in the pH 8.0 and pH 10.0 buffer solutions with 20% TFE (not shown). The absorption of **11** (413 nm in TFE−1% Et_3N) broadened with the addition of the pH 9.0 buffer solution and shifted to 423 nm, and shoulder peaks appeared at 402 and 437 nm (Figure 7B).

The weak Cotton effects of **11** compared to **9** were not due to the weak aggregation property of **11** because its amide-region CD spectra suggested a stable β-sheet structure (Figure 1). The fact that the Cotton effects were the strongest in 30% TFE also suggested that **11** formed a relatively stable assembly. The heptapeptide structure seemed a little too long to take the side-by-side interaction in the assembled structure. Comparing the trimeric

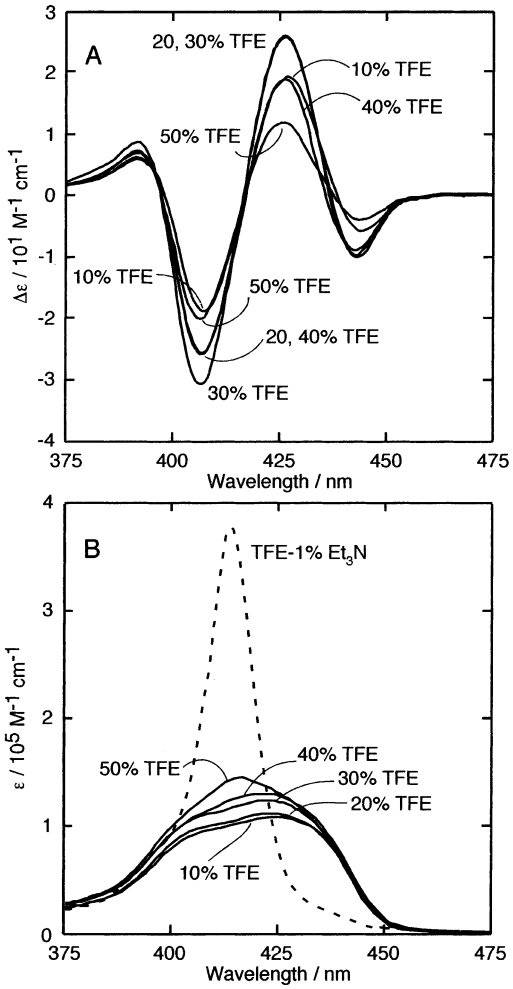

FIGURE 7. (A) CD and (B) UV/vis spectra (Soret region) of **11** (40 μM) in pH 9.0 buffer solution with 10%, 20%, 30%, 40%, and 50% TFE (v/v), and in TFE−1% Et_3N (only in B).

structures of **9** (Figure 4A) and **11** (Figure 6B), the porphyrins of **11** in the neighboring peptide chains (*porphyrins 1* and *2*) were separated than those of **9**. The CD spectra of **11** was not clear yet; however, the main bands ($\Delta\epsilon_{426} = 25.2\ M^{-1}\ cm^{-1}$, $\Delta\epsilon_{408} = -29.7\ M^{-1}\ cm^{-1}$) would be due to the interaction between *porphyrin 1* and *porphyrin 3*. As in the case of **9**, the orientation of *porphyrins 1* and *3* was in the face-to-face orientation; however, the two porphyrins (*porphyrins 1* and *2*) were separated. *The existence of both the side-by-side interaction between porphyrins 1 and 2 and face-to-face interaction between porphyrins 1 and 3 allowed the stable assembly of* ***9****, possibly forming the well-packed porphyrin cluster. The side-by-side interaction seemed to be dominant in* ***10****, the face-to-face interaction in* ***11****, and these conjugates formed a less stable assembly.*

SEC Evidence for the Assembling of 9 and 11. The porphyrins linking the β-sheet peptides **9** and **11** were applied to a size exclusion chromatography (SEC) on a YMC Diol-60 column (the upper resolution limit of this column seemed to be ca. 100 000). With the eluent of the tris buffer solution (5.0 mM, pH 8.0) with 20% CH_3CN, both **9** and **11** eluted before the bovine serum albumin (mol wt 69 000, *A*) eluted (Figure 8, solid circle; see the Experimental Section). Although **9** and **11** eluted in the

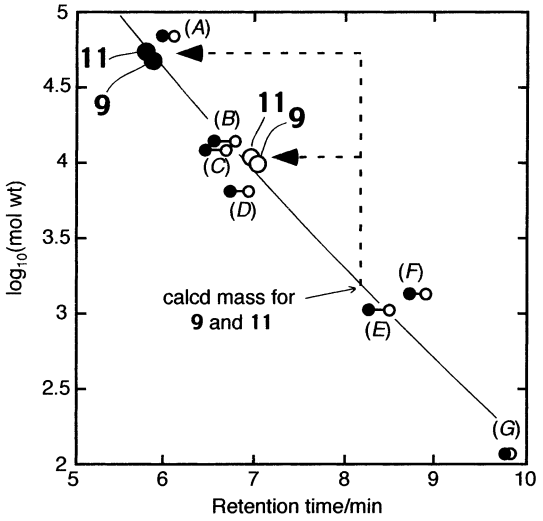

FIGURE 8. SEC analyses of **9** (MW 1332), **11** (MW 1531), and standard proteins (*A*, albumin; *B*, ribonuclease A; *C*, cytochrome C; *D*, aprotinin; *E*, vitamin B_{12}; *F*, angiotensin II; *G*, valine) eluted by (●) pH 8.0 with 20% CH_3CN and (O) pH 7.4 with 20% CH_3CN.

region close to the void volume of the column, their apparent molecular weights were estimated from the calibration curve obtained from the standard proteins: 4.7×10^4 for **9** and 5.3×10^4 for **11**. These porphyrins with β-sheet peptides took the assembled structure with the aggregation numbers of ca. 35 in the SEC analyses. With the eluent of the bis-tris buffer solution (5.0 mM, pH 7.4) with 20% CH_3CN, both **9** and **11** eluted in their oligomer region (Figure 8, open circle), in which their apparent molecular weights were $\sim 1.0 \times 10^4$ (the aggregation numbers were ca. 8). This fact implied that the assembly of **9** and **11** was loose in this eluent (pH 7.4 with 20% CH_3CN), which is consistent with the CD and UV/vis results described above. In fact, the CD spectra of **9** and **11** in this eluent were weak (not shown). The SEC analyses of a low molecular weight sample is sometimes complex because the interaction between the solute and the column surface (diol-modified alkyl groups in this case) cannot be neglected. In fact, **9** or **11** did not elute at all with the pH 9.0 buffer solution (5.0 mM, bis-tris propane) with 20% CH_3CN or the tris buffer solution (10 mM, pH 8.0) with 20% CH_3CN eluent. Under the conditions that **9** and **11** formed large aggregates (pH 9.0 or 10 mM buffer concentration), the aggregates were irreversibly absorbed on the column and did not elute. Nevertheless, the assembling of **9** or **11** in pH 8.0 buffer solution with 20% CH_3CN was directly observed by the SEC analyses. Under the acidic condition at pH 1.7 (15 mM TFA), the self-assembled structure of **9** or **11** was broken and eluted at their monomer region (column, Sephadex Superdex Peptide HR 10/30).

Significantly Broadened ^{1}H NMR Signals of the Porphyrin Protons of 9. The ^{1}H NMR spectrum of **9** was measured at 298 K to further investigate its assembling phenomena. In CD_3OD or in DMSO-d_6, all of the ^{1}H NMR signals of **9** appeared as expected with their chemical shifts, couplings, and signal intensities (Figure 9A, 0.40 mM). Surprisingly, no porphyrin signals were detected in the ^{1}H NMR spectrum of **9** (Figure 9C) in $D_2O-30\%$ CD_3OD (v/v). The peptide moiety of **9** in $D_2O-30\%$ CD_3OD had signals similar to that in CD_3OD except for the signals of NH, for instance, δ 0.99 (Val-γH, 12 H, two doublets), 1.48−1.88 (Lys-β, γ, δH, 12 H, m), and 2.08 (Ac, 3 H, s) in $D_2O-30\%$ CD_3OD and δ 0.95−1.00 (Val-γH), 1.45−1.83 (Lys-β, γ, δH), and 2.08 (Ac, 3 H, s) in CD_3OD. The porphyrin signals observed at δ 8.86 (pyrrole-βH, 8 H), 7.82−8.45 (aromatic-CHs, 16 H), and 2.77 (tolyl-Me, 9 H) in CD_3OD disappeared in $D_2O-30\%$ CD_3OD.

In $H_2O-30\%$ CD_3OD and with use of a pulse sequence (p11) that eliminated the H_2O signal, some signals appeared at δ 8.60, 8.56, 8.43, 8.17, 8.07, 7.80, and 7.19. These signals were assigned as the NH signals (amide-NHs, $-C_6H_4NH-$, Lys-ϵ-NH_3^+, and C-terminal NH_2); however, no porphyrin signals (pyrrole, aromatic-CH, tolyl-*Me*) were observed at all. Thus, the disappearance of the porphyrin signals in $D_2O-30\%$ CD_3OD was not due to the H/D exchange. In fact, a water-soluble porphyrin, tetraphenylporphyrin-*p*,*p*′,*p*″,*p*‴-tetrasulfonic acid, showed the expected porphyrin signals at δ 8.86 (pyrrole-βH) and 8.33/8.26 (d, aromatic-CH) in $H_2O-30\%$ CD_3OD with the same pulse sequence.

In the solvent with a large content of CD_3OD, for instance, in $CD_3OD-10\%$ D_2O, the porphyrin signals were observed with a lower intensity than calculated (Figure 9B). For instance, the pyrrole-H signal appeared at δ 8.86 as a broad peak (a peak width at the half-height was 77 Hz) and the signal intensity was 4.0 H referred to the Val-γH signal of 12 H (Table 2, run 3). The aromatic CH signals appeared at δ 8.19, 8.07, 7.62 and the tolyl-*Me* signal at δ 2.71 in $CD_3OD-10\%$ D_2O; however, these signals were also weak and the signal intensities were about half of the calculated values. Although the assembling of **9** was not observed in the CD and UV/vis spectra in $CH_3OH-10\%$ H_2O, the ^{1}H NMR sample was 10 times more concentrated than the CD and UV/vis samples. Therefore, the decreased signal intensities of the porphyrins would arise from the assembling phenomena of **9**. The porphyrin signals of **9** were extremely broadened in $D_2O-30\%$ CD_3OD via the assembling phenomena and thus hardly detected in the spectra.

With the decrease in the D_2O content, the signal intensities of the pyrrole-βH, aromatic-CHs, and tolyl-*Me* signals gradually recovered (Table 2, runs 2−4). With a decrease in the D_2O content, the pyrrole-βH signals became narrow (see peak width at the half-height); however, the widths of the aromatic-CHs and tolyl-*Me* signals were not drastically changed. The pyrrole-βH signal of **9** in $CD_3OD-5\%$ D_2O became narrow at an elevated temperature, and the peak widths at the half-heights were 42, 28, and 19 Hz at 303, 308, and 313 K, respectively; however, the signal intensities were unchanged (not shown). The peak widths and the signal intensities of the other porphyrin signals were unchanged in this temperature range, while the sample solution became turbid at 318 K. It is noteworthy that the chemical shifts of the porphyrin signals were unchanged at the various D_2O contents and at various temperatures, which suggested that no chemical exchange process was involved. It should be noted here that the chemical shifts of the Cα protons are a useful index for the assignment

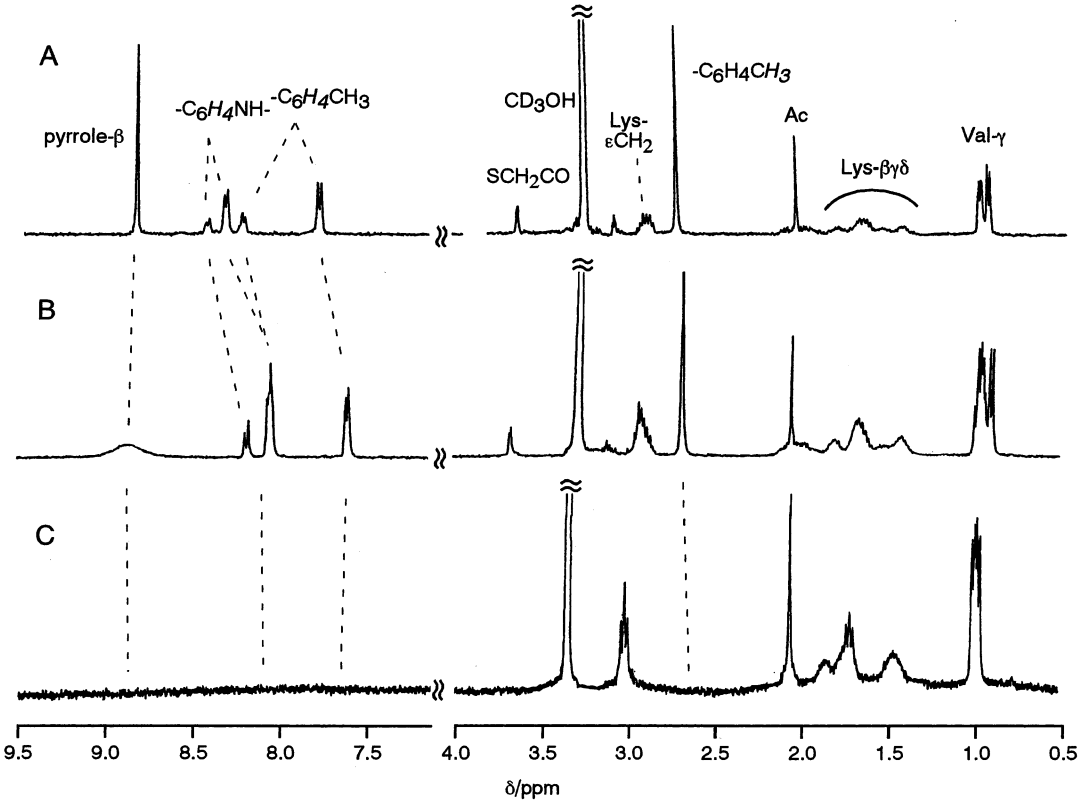

FIGURE 9. ^{1}H NMR (400 MHz) spectra of **9** (0.40 mM) in (A) CD_3OD, (B) $CD_3OD-10\%$ D_2O, and (C) $D_2O-30\%$ CD_3OD (v/v) at 298 K.

TABLE 2. Selected ^{1}H NMR Data for 9 (porphyrin ring protons) in Various Solvents (400 MHz)[a]

		δ/ppm, signal intensity/H (peak width at the half-height/Hz)			
run	solvent[b]	pyrrole-*β*	$-C_6H_4NH-$[c]	$-C_6H_4CH_3$[d]	tolyl-*Me*
1	$D_2O-30\%$ CD_3OD	not detected	not detected	not detected	not detected
2	$CD_3OD-20\%$ D_2O	8.85, 3.3 H (87)	8.18, 0.94 H	7.62, 2.6 H	2.71, 3.9 H (4.4)
3	$CD_3OD-10\%$ D_2O	8.86, 4.0 H (77)	8.19, 1.1 H	7.62, 3.7 H	2.71, 4.8 H (4.4)
4	$CD_3OD-5\%$ D_2O	8.87, 5.0 H (66)	8.19, 1.3 H	7.63, 3.8 H	2.71, 5.5 H (2.6)
5	CD_3OD	8.86, 8.0 H (2.7)	8.45, 2.0 H	7.82, 6.0 H	2.77, 9.0 H (3.1)
6	DMSO-d_6	8.83, 8.0 H (15)	8.15, 2.0 H	7.63[e]	2.66, 9.0 H (2.8)

[a] Measured at 298 K. Signal intensity is referred to Val-*γ*H (12 H). [b] Volume ratio. [c] The protons ortho to porphyrin. [d] The protons meta to porphyrin. [e] Signal overlapped with the other peak.

of the secondary structure of the peptide,[51] as one of the reviewers pointed out. However, the region for the Cα protons was omitted in Figure 9, not only because of the clarity but also because (1) the chemical shifts of Cα protons were solvent-dependent as well as conformation-dependent, therefore, the chemical shifts of Cα protons did not work in this study as the index of the conformation in the spectra shown in Figures 9, and (2) the spectra suffered from the large signal of H_2O derived from the hydrated peptide moiety, thus the signals of Cα protons were sometimes overlapped by the H_2O signal.

The measurements of the ^{1}H NMR relaxation times of **9** (500 MHz) gave further information.[52] The spin−lattice relaxation time T_1 of the pyrrole-*β*H, tolyl-*Me*, Ac, and Val-*γ*H protons were 1.87, 1.12, 1.31, and 0.457 s in CD_3OD, respectively, and were 1.85, 1.21, 1.25, and 0.393 s in $CD_3OD-5\%$ D_2O, respectively. The T_1 values of the porphyrin and peptide protons of **9** only slightly differed in these solvents; however, the spin−spin relaxation time T_2 showed some solvent dependency. The spin−spin relaxation times T_2 of the pyrrole-*β*H, tolyl-*Me*, Ac, and Val-*γ*H protons were 205, 424, 749, and 465 ms in CD_3OD, respectively, and were 104, 386, 650, and 359 ms in $CD_3OD-5\%$ D_2O, respectively. Unfortunately, the pyrrole-*β*H signal was too broad in $CD_3OD-10\%$ D_2O to measure the relaxation times; however, it should be noted that the T_2 value of pyrrole-*β*H became half as large by adding 5% D_2O. The association and the micellar formation of the amphiphilic polymers reportedly caused only slight changes in the T_1 values but decreased the T_2 values.[53] If the addition of D_2O to the CD_3OD solution of **9** induced the hydrophobic interaction between the porphyrins, the porphyrin protons would be in close contact with each other as described above. Then, the spin−spin

(51) Wishart, D. S.; Sykes, B. D.; Richards, F. M. *Biochemistry* **1992**, *31*, 1647.

(52) Palmer, A. G., III; Williams, J.; McDermott, A. *J. Phys. Chem.* **1996**, *100*, 13293. Ruytinx, B.; Berghmans, H.; Adriaensens, P.; Storme, L.; Vanderzande, D.; Gelan, J.; Paoletti, S. *Macromolecules* **2001**, *34*, 522.

relaxation times T_2 were shortened, the signal of the porphyrin rings significantly broadened, and the signal intensities decreased. As for the tolyl-*Me* signal, the T_2 value did not significantly change. The molecular rotation along the porphyrin *meso*-carbon to the aromatic-carbon axis might differ in the situation for the pyrrole-βH protons.

Conclusion

Three conjugates (**9**, **10**, and **11**) of the porphyrin and the acyclic penta- and heptapeptides were synthesized and characterized, in which the porphyrins were linked at the N-terminal Cys. Although the polypeptides **7** and **8** were of the alternative sequence of hydrophilic/hydrophobic amino acids, these short polypeptides showed the CD spectra of a random structure. In contrast, the conjugates of the porphyrin and the polypeptide showed the CD spectra of the β-sheet structure in an aqueous TFE. The porphyrins at the N-terminus of the peptide nucleased the β-sheet formation with the intermolecular interaction between the porphyrins as the driving force. The strong and split Cotton effects were observed for **9**, **10**, and **11** in the CD spectra of the porphyrin Soret-band region. These conjugates showed multiple absorptions in the UV/vis spectra, in which the absorptions broadened with the decrease of TFE. These results showed that the porphyrins are located near each other in the β-sheet structure of the porphyrin−polypeptide conjugates. The CD spectrum of **9** in the porphyrin region was interpreted as the sum of two sets of signals, −/+ in the longwave shifted region and +/− in the shortwave shifted region. Correspondingly, **9** showed multiple UV/vis absorptions. In the polymeric assembly of **9**, two forms of the pair of porphyrins may exist. One set of porphyrins is in the side-by-side interaction of the neighboring peptide chains, which showed the Cotton effect in the longwave shifted region. The other set of porphyrins is in the face-to-face interaction between the first and the third peptide chains, which showed the Cotton effect in the shortwave shifted region. The conjugate linking the porphyrin at the *o*-phenyl position, **10**, showed only the side-by-side interaction of the neighboring peptide chains, probably because of the steric repulsion of the porphyrins. The conjugate linking the porphyrin to the heptapeptide, **11**, predominantly showed the face-to-face interaction between the first and the third peptide chains, probably because the heptapeptide is slightly longer than the porphyrin. The TFE titrations showed the following order of stability of the assembled structure: **9** > **11** > **10**. This result means that both the side-by-side and the face-to-face interactions of the porphyrins (porphyrin cluster) were essential for a stable β-sheet structure. The SEC analyses of the conjugates also showed their assembled structure in the SEC eluents. In the ^{1}H NMR spectrum of **9**, no porphyrin signals were observed in D_2O−30% CD_3OD. In the assembled structure of **9**, the spin−spin relaxation time, T_2, of the hydrophobic porphyrin cluster became shorter, which induced significantly broadened ^{1}H NMR signals.

Experimental Section

UV/vis and CD Spectra. UV/vis and CD spectra were recorded with a quartz cell of 1.0 mm path length. The concentrations of the conjugates in TFE−1% Et_3N (v/v) were determined by using ϵ_{413} = 443 000 M^{-1} cm^{-1} for **9**, ϵ_{414} = 411 000 M^{-1} cm^{-1} for **10**, and ϵ_{413} = 376 000 M^{-1} cm^{-1} for **11**, in which the exact concentrations were determined by the amino acid analyses. The TFE stock solutions of the conjugates were diluted with the appropriate buffer solutions to 40 μM and immediately used for the measurements. The buffer solutions (10 mM) used for the measurements were HEPPSO (pH 8.0), bis-tris propane (pH 9.0), and CAPSO (pH 10.0), in which the pHs were adjusted by aq NaOH or aq HCl and no salts were added.

Analytical Size Exclusion Chromatography. The analytical size exclusion chromatography for the assembled structures of **9** or **11** was carried out by using a YMC−Pack Diol-60 column (0.8 × 30 cm) calibrated with the solutions of albumin (bovine serum, MW 69 000, detection 220 nm), ribonuclease A (bovine pancreas, MW 13 680, detection 220 nm), cytochrome C (horse heart, MW 12 384, detection 420 nm), aprotinin (bovine lung, MW 6512, detection 220 nm), vitamin B_{12} (MW 1355, detection 360 nm), angiotensin II (human, MW 1046, detection 210 nm), and valine (MW 117, detection 210 nm) at a flow rate of 1.0 mL min^{-1}. The buffer solutions (5.0 mM unless otherwise noted) used for the eluents were tris (pH 8.0), bis-tris (pH 7.4), and bis-tris propane (pH 9.0), in which the pHs were adjusted by aq NaOH or aq HCl and no salts were added. The SEC profiles of **9** and **11** eluted by pH 8.0 buffer solution with 20% CH_3CN are given in the Supporting Information.

^{1}H NMR Investigation of the Assembling of 9. ^{1}H NMR spectra of **9** (0.40 mM) were measured in CD_3OD with various contents of D_2O at 298 K unless otherwise noted, using 500- and 400-MHz spectrometers, and the chemical shifts were determined with respect to the internal sodium 3-(trimethylsilyl)propionate-*2,2,3,3-d*$_4$. For the 1D spectra, 256 scans were collected, and for the 2D ^{1}H−^{1}H COSY spectra (field gradient pulse sequence, 400 MHz), 16 scans were collected. For the measurement in H_2O−30% CD_3OD, a p11 pulse sequence (the 1−1 pulse, 400 MHz) was employed. The spin−lattice relaxation time T_1 and the spin−spin relaxation time T_2 were measured at 298 K, using the inversion recovery method and the Carr−Purcell−Meiboom−Gill method,[54] respectively (500 MHz). The variable parameters of 10 were employed and 16 scans were collected for each parameter. The relaxation times T_1 and T_2 were calculated with the linear fitting of the data.

Acknowledgment. We thank Professors Shin Ono at Toyama University and Tamaki Kato at Kyushu Institute of Technology for helpful discussions on the design of the β-sheet peptides, Emeritus Professor Tsutomu Fujimoto and Mr. Kenji Arai at the Kyushu Institute of Technology for the porphyrin syntheses, Ms. Keiko Yamaguchi at the Kyushu Institute of Technology for the FAB-MS measurements, and YMC Corporation for guiding us in the SEC analyses. This study was supported in part by a Grant-in-Aid for Scientific Research (No. 12650869) from the Ministry of Education, Culture, Sports, Science, and Technology, Japan.

Supporting Information Available: Experimental details of the syntheses of **1**−**11**; spectroscopic characterization; ^{1}H NMR spectra; SEC profiles**.** This material is available free of charge via the Internet at http://pubs.acs.org.

JO030001K

(53) Yusa, S.-i.; Kamachi, M.; Morishima, Y. *J. Polym. Sci., Polym. Chem. Ed.* **1999**, *49*, 47. Yamamoto, H.; Tomatsu, I.; Hashidzume, A.; Morishima, Y. *Macromolecules* **2000**, *33*, 7852. Yusa, S.-i.; Sakakibara, A.; Yamamoto, T.; Morishima, Y. *Macromolecules* **2002**, *35*, 5243.

(54) Meiboom, S.; Gill, D. *Rev. Sci. Instrum.* **1958**, *29*, 688.